

Quantification of Retinal and Choriocapillaris Perfusion in Different Stages of Macular Telangiectasia Type 2

Simone Tzaridis,¹ Maximilian W. M. Wintergerst,¹ Clarissa Mai,¹ Tjebo F. C. Heeren,^{2,3} Frank G. Holz,¹ Peter Charbel Issa,⁴ and Philipp Herrmann¹

¹Department of Ophthalmology, University of Bonn, Bonn, Germany

²Moorfields Eye Hospital NHS Foundation Trust, London, United Kingdom

³University College London, Institute of Ophthalmology, London, United Kingdom

⁴Oxford Eye Hospital, Oxford University Hospitals NHS Foundation Trust, and Nuffield Laboratory of Ophthalmology, Department of Clinical Neurosciences, University of Oxford, Oxford, United Kingdom

Correspondence: Simone Tzaridis, Department of Ophthalmology, University of Bonn, Ernst-Abbe-Str. 2, Bonn 53127, Germany; simone.mueller@ukbonn.de.

Submitted: March 8, 2019

Accepted: July 22, 2019

Citation: Tzaridis S, Wintergerst MWM, Mai C, et al. Quantification of retinal and choriocapillaris perfusion in different stages of macular telangiectasia type 2. *Invest Ophthalmol Vis Sci.* 2019;60:3556–3562. <https://doi.org/10.1167/iovs.19-27055>

PURPOSE. To quantify the retinal and choriocapillaris perfusion in different disease stages of macular telangiectasia type 2 (MacTel) using optical coherence tomography-angiography (OCTA).

METHODS. We examined 76 eyes of 76 patients and 24 eyes of 24 age-related controls. Participants underwent multimodal imaging, including OCT and OCTA. Patients' eyes were divided into three groups considering predefined criteria from funduscopy, OCT, and fluorescein angiography, thus reflecting the disease severity ("early," "advanced," and "neovascular"). Quantitative analyses of vessel density (VD), skeleton density (SD), and fractal dimension (FD) were conducted in the superficial and deep retinal plexus and in the avascular layer. The choriocapillaris was analyzed for mean signal intensity and percentage of nondetectable perfused choriocapillaris-area (PNPA).

RESULTS. The deep retinal plexus showed a progressive decrease of mean VD, SD, and FD in the temporal parafovea in all disease stages. In the superficial layer, VD, SD, and FD were significantly decreased in the temporal parafovea of advanced and neovascular stages, while these parameters did not differ from controls in early stages. In MacTel, signals of blood flow were also detectable at the level of the avascular layer and showed a significant increase with disease progression. The choriocapillaris in MacTel showed a significant increase of mean PNPA and a decrease of mean signal intensity in comparison to controls. These findings were consistent in all disease stages.

CONCLUSIONS. Quantitative OCTA data show a progressive rarefaction of the retinal microvasculature in MacTel. We propose an altered choriocapillaris perfusion as a possibly early alteration of the disease.

Keywords: macular telangiectasia type 2, MacTel, optical coherence tomography - angiography, retinal perfusion, choriocapillaris perfusion

Macular telangiectasia (MacTel) type 2 is a bilateral retinal disease that is characterized by both neurodegenerative and vascular alterations, that primarily affect the parafoveal region of the macula.¹ The disease may be diagnosed and graded into five stages according to the system proposed by Gass and Blodi.² However, this classification is not necessarily consecutive and only considers morphological findings from funduscopy and fundus fluorescein angiography (FFA). Recently, novel imaging modalities such as optical coherence tomography (OCT) and OCT-angiography (OCT-A) are gaining in importance for making the diagnosis and assessing the disease severity.³ In this context, the ellipsoid zone (EZ) and its integrity are of particular interest: eyes with MacTel may show a loss of the EZ that usually increases with disease progression and has been shown to be associated with decreased retinal sensitivity.³ The loss of the EZ was thus proposed to serve as a marker of disease severity.^{4,5}

OCT-A is a novel, noninvasive imaging method that shows motion contrast in the retina, and thus can provide detailed

three-dimensional images of the perfused microvasculature in different retinal layers and in the choroid.^{6–11} Previous OCT-A studies of the retinal vasculature in MacTel have observed a decrease of capillary density, dilated and telangiectatic vessels, and the presence of abnormal anastomoses in the outer retina.^{12–14} However, different quantifiable vascular parameters and their changes with disease progression have not yet been systematically investigated, and OCT-A studies on the perfusion of the choriocapillaris remain outstanding.

In this study, we quantify vascular changes in the superficial and deep retinal plexus, in the avascular layer, and in the choriocapillaris of eyes with different disease stages of MacTel using OCTA.

METHODS

In this cross-sectional analysis, consecutive participants with a confirmed diagnosis of MacTel were recruited from the Natural



History and Observation Study (NHOS) from a single center cohort at the Department of Ophthalmology, University Hospital of Bonn, Germany. Protocol details of the study have been published previously.¹⁵ The diagnosis of MacTel type 2 was based on characteristic findings in funduscopy, spectral domain optical coherence tomography (SD-OCT), macular pigment optical density (MPOD), and fundus fluorescein angiography (FFA).¹ Controls were age-matched healthy probands without any evidence of retinal diseases and clear media. Patients and controls underwent a full clinical examination, including best-corrected visual acuity (BCVA) testing, dilated funduscopy, SD-OCT (volume scans of $15^\circ \times 10^\circ$, high resolution mode, 97 scans [Spectralis; Heidelberg Engineering, Heidelberg, Germany]) and OCT-angiography (100k A-scans/second at 1060 nm, macular scans of 3×3 mm formed by 312 horizontal A-scans, with four repeated scans in each fixed location, one volume scan per eye; Zeiss PLEX Elite 9000; Carl Zeiss Meditec, Dublin, CA, USA). OCT-A images were generated using an optical microangiography complex (OMAGc) algorithm.

Inclusion criteria were a complete imaging data set and sufficient imaging quality. The right eye was selected as study eye, unless inclusion criteria were not met. In these cases ($n = 4$), the left eye was selected as study eye.

The study was approved by the local ethics committee of the Friedrich-Wilhelms-University of Bonn, Bonn, Germany, and was conducted in accordance to the tenets of the Declaration of Helsinki. All participants provided informed consent.

Eyes with MacTel were classified according to their disease severity into three groups (“early,” “advanced,” and “neovascular”). Early disease was defined as no visible disruption of the ellipsoid zone on OCT B-scans and no visible pigment changes on funduscopy, but typical findings in FFA, MPOD, and/or in the fellow eye. Eyes with any loss of the EZ on OCT and with or without pigment changes on funduscopy were defined as “advanced,” and eyes with secondary neovascular membranes were defined as “neovascular.”

Image Processing and Analysis

For segmentation of the OCT-A images into superficial, deep, avascular, and choriocapillaris layer, a semiautomated segmentation algorithm was applied, and subsequent manual adjustment of segmentation lines considering individual layer variation and shift in the context of the disease¹⁶ was conducted. Layer segmentation was based on relevant anatomic structures: the superficial layer was defined reaching from the inner boundary of the retinal nerve fiber layer to the outer boundary of the inner plexiform layer (IPL), the deep layer reaching from the outer boundary of IPL to the outer boundary of the outer plexiform layer (OPL), and the avascular layer reaching from the outer boundary of OPL to the outer boundary of the RPE. The latter layer usually does not contain vascular networks in healthy subjects. The choriocapillaris (CC) layer was defined as a slab reaching from 10 to 40 μm below the RPE-fit segmentation. The definitions of the superficial and deep retinal layer correspond to the definition of the superficial and deep retinal plexuses in the current OCT-A nomenclature.¹⁷ OCT-A images were generated using the maximum projection algorithm of the instrument software of each particular slab within the artifact-corrected volume.^{18,19}

Image Postprocessing and Quantitative Analysis

Images of all layers were exported and analyzed using the Fiji software (an expanded version of ImageJ, version 1.51a, available at fiji.sc, provided in the public domain by the

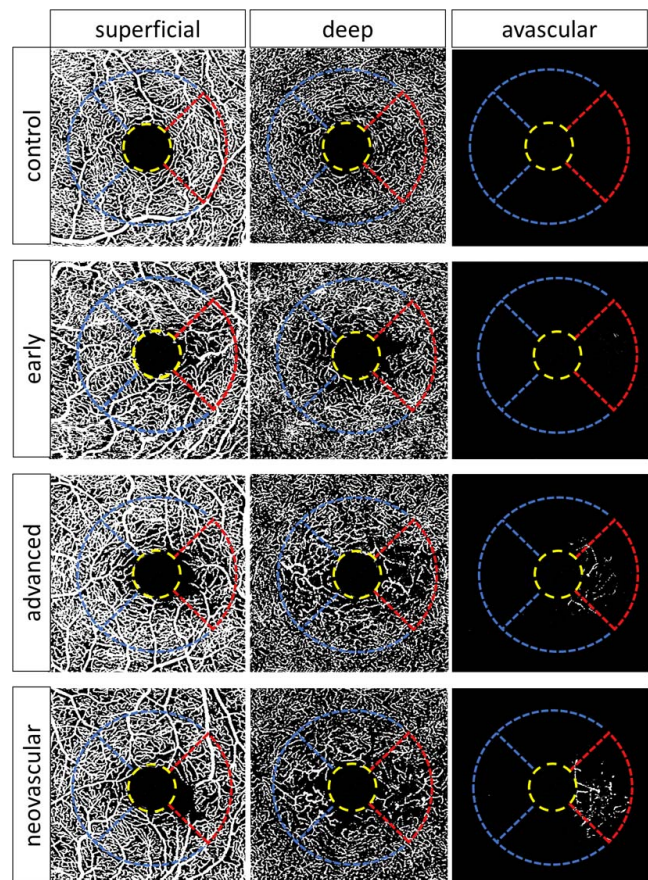


FIGURE 1. Exemplary illustration of the superficial, deep and avascular layer in patient and control eyes (images are postprocessed and binarized). The *red* template indicates the temporal parafoveal area, the *blue* templates indicate the nasal, superior and inferior subfields for quantitative measurements. With disease progression, patient eyes show an increase of intervascular spaces and rarefaction as well as a thickening of small capillaries, resulting in an irregular shape of the foveolar avascular zone. In advanced disease stages, flow signals can be observed at the level of the avascular layer.

National Institute of Health, Bethesda, MD, USA).^{20,21} The superficial and the deep plexus were binarized using the maximum intensity of the foveolar avascular zone as a threshold determined by two masked readers (ST and CM). After binarization, images were skeletonized. Vessel density (VD), skeleton density (SD), and vessel diameter index (VDI) were calculated from the resulting images using the Fiji software as previously described.²² Fractal dimension (FD) was calculated using the box counting method with FracLac, a plug-in for ImageJ (Karperien A, FracLac for ImageJ, available at <http://rsb.info.nih.gov/ij/plugins/fractalac/FLHelp/Introduction.htm>).²³ In MacTel, pathologic alterations usually arise and are most pronounced in the temporal parafovea, predisposing this area to study both early and progressed disease-related changes. In order to determine the position of the temporal parafovea, a customized template following the subfields of the ETDRS-grid (as used in the Early Treatment Diabetic Retinopathy Study)^{24,25} was centered on the foveolar avascular zone. Quantitative analyses of the superficial and deep retinal plexus were primarily conducted in the temporal parafoveal subfield (Fig. 1, indicated in red). The size of this standardized template was customized (Fig. 1: size of the inner, yellow circle: 0.9 mm diameter, size of the outer, red circle: 2.4 mm diameter) in order to fit into the borders of the image and include the area

of interest. In cases, where the FAZ was irregularly distorted (e.g., in eyes with progressed disease stages), the center of the FAZ was determined following neighboring vessels of the nasal, superior and inferior parafovea. In a secondary analysis, quantitative measures were also conducted within the nasal, inferior and superior parafoveal subfields (Fig. 1, indicated in blue). For binarization of the avascular layer, the borders of the FAZ were projected within the avascular layer and thresholding was conducted using the maximum intensity that was determined within this area (see Supplementary Fig. S1, the projection of the FAZ is indicated with a yellow-dotted outline). The avascular layer usually does not show signals of blood flow in healthy subjects. Vessel density (VD) was subsequently calculated from the resulting complete image (3 × 3 mm) using the FIJI software as previously described.^{20,22}

The CC-slab was analyzed for mean signal intensity, kurtosis and percentage of nondetectable perfused CC-area (PNPA) as previously described.^{26,27} In brief, images were binarized using the Phansalkar method (radius of 50 pixels). Subsequently, the “Analyze particles” command of FIJI enabled to count and assess the size of all areas containing an absence of flow information (“flow voids”) as a percentage of the nondetectable perfused area (PNPA).²⁸ Kurtosis is a statistical parameter that can be used in order to describe the signal intensity distribution of a grey-level image.^{29,30} Its application for characterizing the frequency of intensity values in CC-sections of OCT-A images has previously been described.²⁷ In neovascular eyes, the exact localization and extension of neovascular membranes was determined, and the respective area was excluded from the quantitative CC-analyses.

Statistical Analysis

Statistical analysis was performed using graphing software (GraphPad Prism, version 7.05; GraphPad Software, San Diego, CA, USA). Continuous variables were described by using the mean ± standard deviation and categorical variables were analyzed using frequency tables. For intergroup comparisons 1-way ANOVA with Bonferroni correction for multiple testing was computed, unless otherwise indicated. Intraclass correlation was used in order to assess interreader reliability for the determination of the maximum intensity within the FAZ. A *P* value <0.05 was accepted as statistically significant.

RESULTS

Data of 76 eyes of 76 patients (mean age of 62.3 years ± SD 6.1; range, 49–78) and 24 eyes of 24 age-matched controls (mean age of 61.5 years ± SD 5.9; range, 46–75) were included in this analysis. We graded 18 eyes as early, 45 as advanced and 13 as neovascular.

With disease progression, eyes with MacTel showed an increase of intervacular spaces and rarefaction of vessels as well as a thickening of parafoveal capillaries, resulting in an irregular shape of the foveolar avascular zone. These alterations were present both in the superficial and deep retinal plexus and were most pronounced in the temporal parafovea. In eyes with advanced disease stages, flow signals were also observed at the level of the avascular layer. Examples of the superficial, deep and avascular layer in patient and control eyes are shown in Figure 1.

Quantitative assessments in the temporal sector of the superficial plexus revealed a significant decrease of mean VD, SD, and FD in eyes with advanced and neovascular disease stages, respectively (in comparison to controls all *P* < 0.001; Fig. 2). In early stages, however, these parameters did not differ from controls.

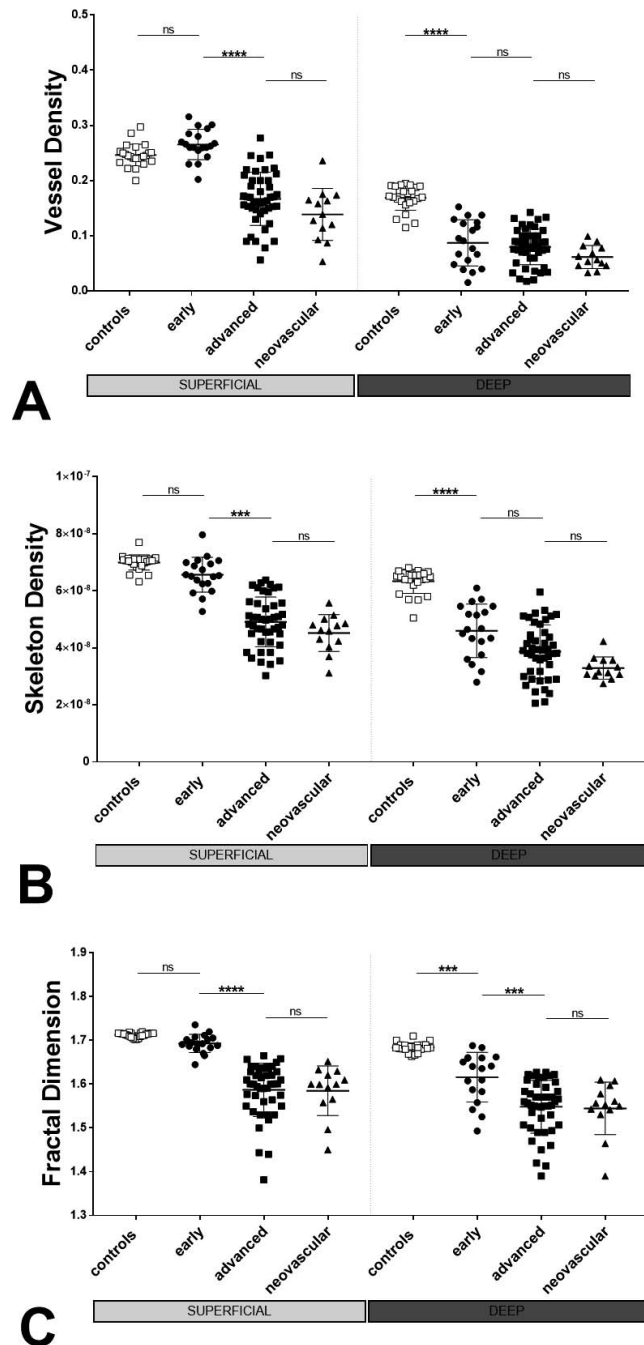


FIGURE 2. Quantitative measures (single values, mean values and standard deviations) of vessel density (A), skeleton density (B), and fractal dimension (C) in the superficial and deep plexus of MacTel and control eyes. In the deep plexus, all parameters show a decrease in patients. In the superficial plexus, eyes with advanced and neovascular stages show a significant decrease of all parameters, while eyes with early stages do not differ from controls. Controls: *n* = 24; patients: early: *n* = 18; progressed: *n* = 45; neovascular: *n* = 13. NS, no significant difference. ****P* < 0.001. *****P* < 0.0001.

In the temporal sector of the deep plexus, all groups showed a significant decrease of mean VD, SD, and FD (all *P* < 0.001) in comparison to controls, that further decreased with disease progression. Quantitative data (mean values ± standard deviations) for measurements within the temporal parafovea are shown in Figure 2 and listed in the Table of the supplement.

TABLE. Quantitative Data (mean values ± SD) of Choriocapillaris Perfusion Parameters

	PNPA [%]		Kurtosis		Signal Intensity	
	Mean ± SD	P Value*	Mean ± SD	P Value*	Mean ± SD	P Value*
Controls	17.7 ± 3.8	NA	1.77 ± 0.7	NA	209.8 ± 11.1	NA
Early	30.1 ± 3.5	<0.001	-1.17 ± 0.6	<0.0001	177.3 ± 15.2	<0.001
Advanced	32.1 ± 3.4	<0.001	-1.40 ± 0.3	<0.0001	173.1 ± 10.7	<0.0001
Neovascular	34.3 ± 4.1	<0.0001	-1.43 ± 0.4	<0.0001	166.5 ± 15.3	<0.0001

Parameters include the percentage of nondetectable perfused area (PNPA), mean signal intensity, and kurtosis of signal intensity distribution) in patients and controls.

* The listed P values describe the significances of differences between each disease stage (early, advanced, neovascular) and controls (1-way ANOVA test with Bonferroni correction for multiple testing).

In a comparative analysis quantitative measures within the nasal, superior, inferior, and temporal parafoveal sectors were compared between patients and controls. In addition to the above reported changes within the temporal sector, significant differences between patients and controls were only found for the nasal sector of the deep plexus in eyes with advanced and neovascular stages, respectively. Here, we found a significant decrease of VD, SD, and FD in comparison to control eyes (all $P < 0.01$; Supplementary Figure S2).

At the level of the avascular layer, signals of blood flow were only observed in eyes with advanced disease stages (Fig. 1). A quantitative analysis of these changes (VD only) revealed a significant increase of mean VD in eyes with advanced and neovascular stages, respectively (for both $P < 0.001$, see Supplementary Table S1). Though in some eyes with early disease stages single signals of blood flow were detectable within the avascular layer, the difference to control eyes,

where the avascular layer showed no signal at all, was not significant.

The quantitative analysis of the CC revealed a significantly reduced mean signal intensity as well as a reduced kurtosis of signal intensity distribution in all groups of MacTel eyes (all $P < 0.001$), indicating a more heterogenous OCTA signal with a wider distribution (Table; Fig. 3; Supplementary Fig. S3). Furthermore, there were more choriocapillaris perfusion flow-voids (indicated by a significant increase of mean PNPA; all $P < 0.001$; Fig. 3C) in MacTel eyes compared to controls. Notably, among our patients, we found no significant differences between eyes of early, advanced and neovascular stages, respectively (Figs. 3B–D). Quantitative data of CC perfusion parameters are shown in the Table. Interestingly, in eyes with neovascular stages, a focal increase of flow voids was observed surrounding neovascular membranes (Fig. 4).

Interreader agreement was high for the determination of thresholds for binarization of the superficial, deep, and

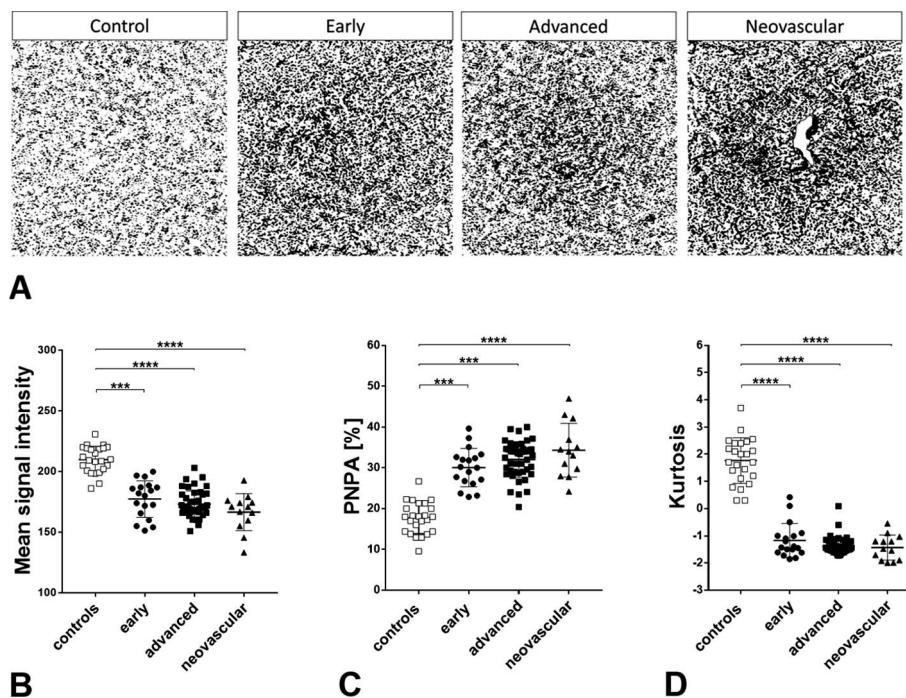


FIGURE 3. (A) Exemplary illustration of the choriocapillaris layer in controls and patients. Patients show an overall increase of flow voids that seems to be present in all disease stages. In the neovascular eye, the neovascular membrane is marked as white area, that was excluded from the quantitative analysis. (B–D) Quantification of mean signal intensity (B), percentage of nondetectable perfused area (PNPA; [C]), and kurtosis of signal intensity distribution (D) in the choriocapillaris layer of patients and controls. The mean PNPA is significantly increased, while the mean signal intensity and kurtosis are significantly decreased in all disease stages in comparison to controls (*** $P < 0.001$, **** $P < 0.0001$).

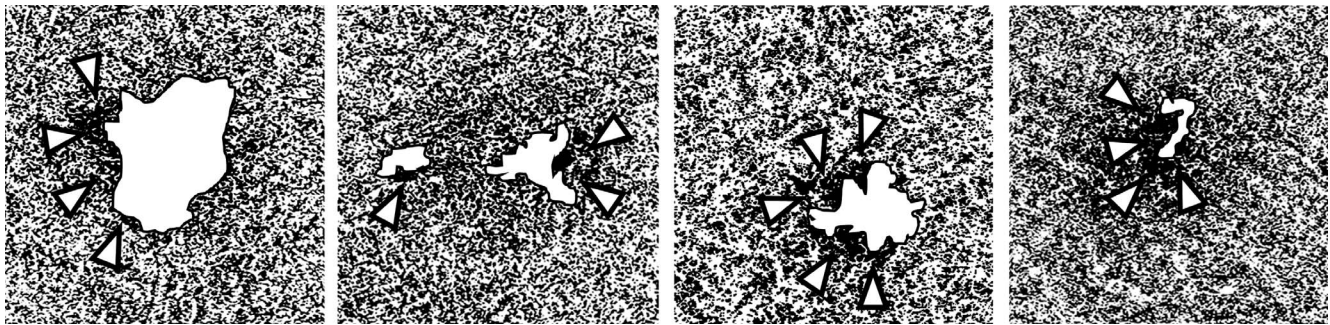


FIGURE 4. Exemplary illustration of choriocapillaris sections of eyes with neovascular disease stages. Neovascular membranes are marked as white areas. Note the increase of flow voids in the perimembranous zone, indicated with *white arrowheads*.

avascular retinal layers (intraclass correlation coefficients and confidence intervals: superficial layer: 0.84; 0.80–0.94; deep layer: 0.87; 0.77–0.9; and avascular layer: 0.81; 0.79–0.9).

DISCUSSION

Although MacTel was lately considered to be possibly a primarily neurodegenerative disease, it is also characterized by its vascular alterations. While characteristic vascular changes in funduscopy and fluorescein angiography may help to make the diagnosis, OCTA allows to differentiate, allocate, and quantify vascular changes within different retinal layers and the choroid.^{6–11} Previous studies showed a decrease of mean capillary density and rarefaction in both superficial and deep retinal plexus in eyes with MacTel.^{12,13,31} It was suggested that vascular changes might first arise in the deep layer, and only later in the disease course extend to the superficial layer and outer retina. However, so far, neither longitudinal data nor a systematic analysis of eyes with different stages was available supporting this hypothesis. In this study, we showed a progressive rarefaction of vessels in the temporal parafovea of the deep retinal plexus indicated by a significant decrease of vessel and skeleton density in all disease stages. In the superficial plexus, however, a decrease of vessel and skeleton density within the temporal parafovea was only detectable in eyes with advanced and neovascular stages, while early stages did not differ from controls. This finding supports that earliest vascular changes arise in the deep plexus, while visible alterations in the superficial plexus may be considered a sign of more advanced disease. While in the superficial plexus changes were limited to the temporal parafovea, a decrease of vessel and skeleton density was also observed within the nasal parafovea of the deep plexus of eyes with advanced and neovascular stages. This may be explained by the known extension of morphological changes to the nasal parafovea with disease progression,^{32–34} and further supports the hypothesis of changes to arise in the deep plexus first.

In line with recent findings,^{12,35} we observed the presence of pathologic vascular structures in the avascular layer of eyes with advanced and neovascular disease stages, but not in early stages. Though different studies proposed a descent of vascular changes to the outer retina,^{12,35,36} segmentation of retinal layers in eyes with advanced disease stages may be challenging, and a collapse of retinal layers due to increasing atrophy may at least in part be responsible for the observed phenomenon.

While alterations of the retinal vasculature have long been known, the role of vascular changes in the choriocapillaris and choroid in MacTel is still obscure. The involvement of choroidal vessels in the context of secondary NVs in MacTel has been controversially discussed.^{36–39} In a recent qualitative analysis, we showed an increase of flow voids and irregular

appearance of the choriocapillaris in eyes with advanced (but non-proliferative) disease stages.³⁶ In this study, we quantified these changes and found an overall reduced and more irregular perfusion of the choriocapillaris indicated by a significant increase of flow voids and reduced kurtosis of signal intensity distribution. Notably, these findings were already observed in early disease stages, indicating an earlier affection of the choroid than previously expected. Though changes of CC perfusion seemed to be most pronounced within the central parafoveal region to which morphologic alterations are usually limited in MacTel, they also seemed to extend beyond this area, thus implying an overall broader affection of the choriocapillaris. Interestingly, in eyes with neovascular disease stages, we observed a pronounced focal increase of flow voids surrounding neovascular membranes. Though a hypoperfusion of the choriocapillaris may be considered a new and intriguing finding in MacTel, these findings must be interpreted with caution. Superimposing structures, and especially dense pigment plaques and prominent vessels, may cause shadowing artefacts and may thus enhance the impression of an altered structure of the choriocapillaris. Furthermore, in general, imaging of the choriocapillaris *in vivo* is still challenging and movement artefacts and speckle noise may influence image quality. Nevertheless, a hypoperfusion and possibly resulting hypoxia of the choriocapillaris might represent a conceivable trigger factor for a shift of retinal vessels to the outer retina, and the development and growth of neovascularizations in eyes with MacTel.

Study Limitations

This study was conducted in a cross-sectional manner. Future collection of longitudinal data is needed in order to verify our results.

Furthermore, our data were not corrected for axial length variations and resulting retinal magnification. Though, refraction errors were overall low in our proband cohort and did not differ between patients and controls (patients: median refraction error: +0.75 diopters (range, –3.5 to +3.75 diopters) and controls: median: +0.5 diopters (range, –4.0 to +3.5 diopters), axial length variations might have influenced our results.

The occurrence of atrophy and NV-associated changes resulting in an altered retinal architecture complicates the segmentation of OCT images and causes imaging artefacts that may influence the test results in spite of careful review and manual correction of segmentation. Furthermore, shadowing artefacts of large vessels and pigment plaques may impede the evaluation of subjacent structures (especially in the avascular and choriocapillaris layer), though an algorithm subtracting artefacts caused by superimposing structures was applied, and

areas with dense structures (e.g., neovascular membranes) were excluded from the quantitative analysis of the CC layer.

CONCLUSIONS

We provide quantitative OCT-A data showing a rarefaction of the microvasculature in the superficial and deep retinal plexus, that increases with disease progression in eyes with MacTel. We propose an altered choriocapillaris perfusion as a possibly early alteration in MacTel.

Acknowledgments

Supported by the Lowy Medical Research Institute, La Jolla, CA, USA; German Research Foundation (Research grant, project number: 406053827), BONFOR GEROK Program, Faculty of Medicine, University of Bonn, (Grant No O-137.0028, MW), ProRetina, Bonn, Germany, and the National Institute for Health Research (NIHR) Oxford Biomedical Research Centre (BRC), Oxford, United Kingdom. The views expressed are those of the authors and not necessarily those of the NHS, the NIHR, or the Department of Health.

Disclosure: S. Tzaridis, None; M.W.M. Wintergerst, None; C. Mai, None; T.F.C. Heeren, None; F.G. Holz, None; P. Charbel Issa, None; P. Herrmann, None

References

- Charbel Issa P, Gillies MC, Chew EY, et al. Macular telangiectasia type 2. *Prog Retin. Eye Res.* 2013;34:49-77.
- Gass JD, Blodi BA. Idiopathic juxtafoveolar retinal telangiectasis. Update of classification and follow-up study. *Ophthalmology.* 1993;100:1536-1546.
- Heeren TFC, Kitka D, Florea D, et al. Longitudinal correlation of ellipsoid zone loss and functional loss in macular telangiectasia type 2. *Retina.* 2018;38(suppl 1):S20-S26.
- Runkle AP, Kaiser PK, Srivastava SK, Schachat AP, Reese JL, Ehlers JP. OCT angiography and ellipsoid zone mapping of macular telangiectasia type 2 from the AVATAR Study. *Invest Ophthalmol Vis Sci.* 2017;58:3683-3689.
- Peto T, Heeren TFC, Clemons TE, et al. Correlation of clinical and structural progression with visual acuity loss in macular telangiectasia type 2: MacTel Project Report No. 6. The MacTel Research Group. *Retina.* 2018;38(suppl 1):S8-S13.
- Spaide RF, Fujimoto JG, Waheed NK. Optical coherence tomography angiography. *Retina.* 2015;35:2161-2162.
- Choi W, Mohler KJ, Potsaid B, et al. Choriocapillaris and choroidal microvasculature imaging with ultrahigh speed OCT angiography. *PLoS One.* 2013;8:e81499.
- Kim DY, Fingler J, Zawadzki RJ, et al. Optical imaging of the chorioretinal vasculature in the living human eye. *Proc Natl Acad Sci U S A.* 2013;110:14354-14359.
- Wang RK. Optical microangiography: a label free 3D imaging technology to visualize and quantify blood circulations within tissue beds in vivo. *IEEE J Sel Top Quantum Electron.* 2010;16:545-554.
- Wang RK, An L, Francis P, Wilson DJ. Depth-resolved imaging of capillary networks in retina and choroid using ultrahigh sensitive optical microangiography. *Opt Lett.* 2010;35:1467-1469.
- Wang RK, Jacques SL, Ma Z, Hurst S, Hanson SR, Gruber A. Three dimensional optical angiography. *Opt Express.* 2007;15:4083-4097.
- Chidambara L, Gadde SG, Yadav NK, et al. Characteristics and quantification of vascular changes in macular telangiectasia type 2 on optical coherence tomography angiography. *Br J Ophthalmol.* 2016;100:1482-1488.
- Spaide RF, Klancnik JM Jr, Cooney MJ. Retinal vascular layers in macular telangiectasia type 2 imaged by optical coherence tomographic angiography. *JAMA Ophthalmol.* 2015;133:66-73.
- Thorell MR, Zhang Q, Huang Y, et al. Swept-source OCT angiography of macular telangiectasia type 2. *Ophthalmic Surg Lasers.* 2014;45:369-380.
- Clemons TE, Gillies MC, Chew EY, et al. Baseline characteristics of participants in the natural history study of macular telangiectasia (MacTel) MacTel Project Report No. 2. *Ophthalmic Epidemiol.* 2010;17:66-73.
- Spaide RF, Curcio CA. Evaluation of segmentation of the superficial and deep vascular layers of the retina by optical coherence tomography angiography instruments in normal eyes. *JAMA Ophthalmol.* 2017;135:259-262.
- Campbell JP, Zhang M, Hwang TS, et al. Detailed vascular anatomy of the human retina by projection-resolved optical coherence tomography angiography. *Sci Rep.* 2017;7:42201.
- Spaide RF, Fujimoto JG, Waheed NK. Image artifacts in optical coherence tomography angiography. *Retina.* 2015;35:2163-2180.
- Zhang Q, Zhang A, Lee CS, et al. Projection artifact removal improves visualization and quantitation of macular neovascularization imaged by optical coherence tomography angiography. *Ophthalmol Retina.* 2017;1:124-136.
- Schindelin J, Arganda-Carreras I, Frise E, et al. Fiji: an open-source platform for biological-image analysis. *Nat Methods.* 2012;9:676-682.
- Schneider CA, Rasband WS, Eliceiri KW. NIH Image to ImageJ: 25 years of image analysis. *Nat Methods.* 2012;9:671-675.
- Kim AY, Rodger DC, Shahidzadeh A, et al. Quantifying retinal microvascular changes in uveitis using spectral-domain optical coherence tomography angiography. *Am J Ophthalmol.* 2016;171:101-112.
- Masters BR. Fractal analysis of the vascular tree in the human retina. *Annu Rev Biomed Eng.* 2004;6:427-452.
- Early Treatment Diabetic Retinopathy Study Research Group. Photocoagulation for diabetic macular edema. Early Treatment Diabetic Retinopathy Study report number 1. *Arch Ophthalmol.* 1985;103:1796-1806.
- Early Treatment Diabetic Retinopathy Study Research Group. Grading diabetic retinopathy from stereoscopic color fundus photographs—an extension of the modified Airlie House classification. ETDRS report number 10. *Ophthalmology.* 1991;98(5 Suppl):786-806.
- Spaide RF. Choriocapillaris flow features follow a power law distribution: implications for characterization and mechanisms of disease progression. *Am J Ophthalmol.* 2016;170:58-67.
- Wintergerst MWM, Pfau M, Muller PL, et al. Optical coherence tomography angiography in intermediate uveitis. *Am J Ophthalmol.* 2018;194:35-45.
- Borrelli E, Uji A, Sarraf D, Sadda SR. Alterations in the choriocapillaris in intermediate age-related macular degeneration. *Invest Ophthalmol Vis Sci.* 2017;58:4792-4798.
- Arab A, Wojna-Pelczar A, Khairnar A, Szabo N, Ruda-Kucerova J. Principles of diffusion kurtosis imaging and its role in early diagnosis of neurodegenerative disorders. *Brain Res Bull.* 2018;139:91-98.
- Jensen JH, Helpert JA. MRI quantification of non-Gaussian water diffusion by kurtosis analysis. *NMR Biomed.* 2010;23:698-710.
- Thorell MR, Zhang Q, Huang Y, et al. Swept-source OCT angiography of macular telangiectasia type 2. *Ophthalmic Surg Lasers Imaging Retina.* 2014;45:369-380.
- Charbel Issa P, Helb HM, Rohrschneider K, Holz FG, Scholl HP. Microperimetric assessment of patients with type 2 idiopathic

- macular telangiectasia. *Invest Ophthalmol Vis Sci.* 2007;48:3788-3795.
33. Barthelmes D, Gillies MC, Sutter FK. Quantitative OCT analysis of idiopathic perifoveal telangiectasia. *Invest Ophthalmol Vis Sci.* 2008;49:2156-2162.
 34. Abujamra S, Bonanomi MT, Cresta FB, Machado CG, Pimentel SL, Caramelli CB. Idiopathic juxtafoveal retinal telangiectasis: clinical pattern in 19 cases. *Ophthalmologica.* 2000;214:406-411.
 35. Spaide RF, Yannuzzi LA, Maloca PM. Retinal-choroidal anastomosis in macular telangiectasia type 2. *Retina.* 2018;38:1920-1929.
 36. Tzaridis S, Heeren T, Mai C, et al. Right-angled vessels in macular telangiectasia type 2 [published online February 26, 2019]. *Br J Ophthalmol.* <https://doi.org/10.1136/bjophthalmol-2018-313364>.
 37. Zhang Q, Wang RK, Chen CL, et al. Swept source optical coherence tomography angiography of neovascular macular telangiectasia type 2. *Retina.* 2015;35:2285-2299.
 38. Yannuzzi LA, Bardal AM, Freund KB, Chen KJ, Eandi CM, Blodi B. Idiopathic macular telangiectasia. *Arch Ophthalmol.* 2006;124:450-460.
 39. Davidorf FH, Pressman MD, Chambers RB. Juxtafoveal telangiectasis-a name change? *Retina.* 2004;24:474-478.